

NEW INFORMATION ON THE CRANIAL MORPHOLOGY OF *AVIMIMUS* (THEROPODA: OVIPTOROSAURIA)

TAKANOBU TSUIHIJI,*¹ LAWRENCE M. WITMER,² MAHITO WATABE,³ RINCHEN BARSBOLD,⁴
KHISHIGJAV TSOGTBAATAR,⁴ SHIGERU SUZUKI,⁵ and PUREVDORJ KHATANBAATAR⁴

¹Department of Earth and Planetary Science, The University of Tokyo, 7-3-1 Hongo, Bunkyo-ku, Tokyo 113-0033, Japan,
ttsuihiji@eps.s.u-tokyo.ac.jp;

²Department of Biomedical Sciences, Heritage College of Osteopathic Medicine, Ohio University, Athens, Ohio 45701, U.S.A.,
witmerL@ohio.edu;

³School of International Liberal Studies, Waseda University, 1-6-1 Nishiwaseda, Shinjuku-ku, Tokyo 169-8050, Japan,
mahitow@gmail.com;

⁴Institute of Paleontology and Geology, Mongolian Academy of Sciences, Sambuu Street, Chingeltei Distric-4, Ulaanbaatar 14201,
Mongolia, maspaleo@yahoo.com; tsogtmondin@gmail.com; shinehoo_kh@yahoo.com;

⁵Hayashibara Co., Ltd., 1-1-3 Shimoishii, Okayama 700-0907, Japan, shigeru.suzuki@hb.nagase.co.jp

ABSTRACT—The cranial morphology of the oviraptorosaurian *Avimimus portentosus* is described based on a new specimen, one that includes bones such as the nasal and the jugal, which had not been available or only incompletely preserved previously. The left and right nasals are fused together as in oviraptorids. Morphology of the jugal, which is not fused with the quadratojugal, and the postorbital indicate that the infratemporal fenestra is completely separate from the orbit, not confluent with the latter, as inferred previously. The left and right dentaries are fused together without a trace of suture. Such newly available information indicates that the skull of *Avimimus* is not as ‘avian’-like as inferred in previous studies. Rather, it shows a mixture of plesiomorphic and derived character states observed in Oviraptorosauria, consistent with an intermediate phylogenetic position of this dinosaur between Early Cretaceous basal oviraptorosaurians and the diverse clade of Caenagnathoidea.

Citation for this article: Tsuihiji, T., L. M. Witmer, M. Watabe, R. Barsbold, K. Tsogtbaatar, S. Suzuki, and P. Khatanbaatar. 2017. New information on the cranial morphology of *Avimimus* (Theropoda: Oviraptorosauria). *Journal of Vertebrate Paleontology*. DOI: 10.1080/02724634.2017.1347177.

INTRODUCTION

The oviraptorosaurian *Avimimus portentosus* is known for possessing ‘avian’-like features (Kurzanov, 1981, 1985, 1987; Osmólska, 1981; Vickers-Rich et al., 2002). In addition to postcranial characteristics such as the presence of a carpometacarpus (semilunate carpal fused with three metacarpals), a tarsometatarsus (distal tarsals fused with metatarsals), and a tibiotarsus (fusion between the tibia and the proximal tarsals), Kurzanov (1985, 1987) described ‘avian’-like features in the skull, including fusion of bones constituting the braincase and a dome-like, inflated skull roof, and also inferred the presence of an incomplete lower temporal fenestra confluent with the orbit. However, the cranial materials available to Kurzanov (1985, 1987) were limited to two braincases, one of which preserved a fairly complete neurocranium with palatal bones and other surrounding bones fused together, fused left and right premaxillae, a fragmentary dentary, and fused postdentary bones. Despite these specimens providing tantalizing clues about a potentially bird-like skull, the entire configuration of the skull of *Avimimus* remained unknown. Since the early 2000s, however, additional specimens of *Avimimus* have been found in the Upper Cretaceous of the Gobi Desert (e.g., Watabe et al., 2000; Currie et al., 2008). Among such findings, new information on the skull, especially the nasals, that had not been available to Kurzanov (1985,

1987), was recently provided by Funston et al. (2016), clarifying various aspects of the cranial anatomy of *Avimimus*. However, detailed information on some parts of the skull, such as the temporal region, is still lacking for this taxon.

In this paper, we provide detailed description of cranial bones of a new specimen of *Avimimus* collected at the Bugin (Bügiin) Tsav locality during the Hayashibara Museum of Natural Sciences–Mongolian Paleontological Center (now Institute of Paleontology and Geology) Joint Expedition in the western Gobi Desert in 2006. The specimen is an associated skeleton that includes the braincase and several other disarticulated, but associated, cranial bones in addition to various postcranial bones. A particular emphasis in this paper is on confirming or testing the presence of ‘avian’-like characteristics that Kurzanov (1985, 1987) described or postulated. In addition, the phylogenetic distribution of cranial characters in Oviraptorosauria is assessed by incorporating new information available on the present specimen in a previously published data matrix, providing new insight into the evolutionary sequence of cranial characteristics in Oviraptorosauria.

Institutional Abbreviations—MPC, Institute of Paleontology and Geology, Mongolian Academy of Sciences, Ulaanbaatar, Mongolia; PIN, Paleontological Institute, Russian Academy of Sciences, Moscow, Russia.

Anatomical Abbreviations—I, grooves for the olfactory nerves; II, optic nerve foramen; V, trigeminal nerve foramen; XII, hypoglossal nerve foramen; **alpf**, anterolateral articular

*Corresponding author.

process of the frontal; **aocm**, atlanto-occipital capsular membrane; **ar**, anterior ramus; **?asf**, putative articular surface for the frontal; **?asj**, putative articular surface for the jugal; **asl**, articular surface for the lacrimal; **asm**, articular surface for the maxilla; **?aspm**, putative articular surface for the premaxilla; **aspo**, articular surface for the postorbital; **assp**, articular surface for the splenial; **b**, boss; **bc**, attachment of m. biventer cervicis; **bsi**, basal sinus; **bt**, basal tubera; **c**, attachment of m. complexus; **cmcv**, foramen for the caudal middle cerebral vein; **co**, part of the coronoid or coronoid-articular-surangular complex; **cs**, attachment of m. capitisternalis; **dep**, depression; **dm**, m. depressor mandibulae; **ep**, possible fused epipterygoid; **f**, frontal; **fa**, foramina; **fm**, foramen magnum; **fv**, fenestra vestibuli; **j**, jugal (left side); **jf**, jugular foramen; **lapf**, lateral articular process of the nasals for the frontal; **ld**, lateral depression (the articular surface for the lacrimal) on the anterolateral process of frontal; **lppm**, lateral articular process of the nasals for the premaxilla; **lppt**, lateral process of the pterygoid; **lr**, lingual ridge; **ls**, laterosphenoid; **lv**, longitudinal vascular groove; **mapf**, medial articular processes of the nasals for the frontal; **md**, medial depression (the articular surface for the nasal) on the anterolateral process of frontal; **mg**, Meckelian groove; **mpf**, median articular processes of the frontal; **mppm**, median articular process of the nasals for the premaxilla; **mppt**, medial process of the pterygoid; **n**, nasal (fragment); **oc**, occipital condyle; **p**, parietal; **paroc**, paroccipital process; **pf**, pituitary fossa; **pnf**, putative pneumatic fossa; **po**, postorbital; **pr**, posterior ramus; **prm**, prominence; **pro**, prootic; **psr**, parasphenoidal rostrum; **q**, quadrate; **qc**, quadrate articular condyle for the articular; **qj**, quadratojugal; **r**, ridge; **red**, attachment of m. rectus capitis dorsalis; **rcl**, attachment of m. rectus capitis lateralis; **rcv**, attachment of m. rectus capitis ventralis; **rd**, round depression; **s**, slit for articulation for the nasal; **scl**, attachment of m. splenius capitis, lateral part; **scm**, attachment of m. splenius capitis, medial part; **ss**, attachment of the supraspinal ligament.

MATERIALS AND METHODS

Cladistic analyses were conducted with equally weighted parsimony using TNT 1.0 (Goloboff et al., 2008). One thousand replicates of Wagner trees (using random addition sequence) followed by tree bisection and reconnection branch swapping were run holding 10 trees per replicate with all zero-length branches collapsed. Because some replicates encountered more than 10 most parsimonious trees, further branch swapping starting from the most parsimonious trees in memory was conducted. Branch support was estimated with bootstrap (1000 replicates) and Bremer support values.

In the present study, names of muscles attaching to the occipital region of the skull follow the avian terminology proposed by Vanden Berge and Zweers (1993). This usage does not necessarily imply that *Avimimus* would have possessed the avian condition. Any nomenclature that has been used for these clades could be used for indicating muscles reconstructed in non-avian dinosaurs because neck muscles attaching to the occiput are mostly conserved among birds, crocodylians, and lepidosaurians and the homologies are well understood (e.g., Tsuihiji, 2010). The avian myological nomenclature is chosen here partly because of phylogenetic proximity of Aves and oviraptorosaurians but mostly because it is readily available in a single comprehensive volume—*Nomina Anatomica Avium*—in which anatomical terms are unambiguously defined (Baumel et al., 1993).

SYSTEMATIC PALEONTOLOGY

DINOSAURIA Owen, 1842
THEROPODA Marsh, 1881
MANIRAPTORA Gauthier, 1986

OVIRAPTOROSAURIA Barsbold, 1976
AVIMIMUS PORTENTOSUS Kurzanov, 1981
(Figs. 1–10)

Holotype—PIN 3907-1, occipital region of the skull, cervical and dorsal vertebrae, partial forelimb skeleton, fragmentary pelvic girdle, and mostly complete hind limb skeleton.

Type Locality and Horizon—Shar Tsav, eastern Gobi Desert, Mongolia; Nemegt Formation; late Campanian–early Maastrichtian to Maastrichtian.

Referred Material—MPC-D 100/125, associated, partially articulated skeleton; MPC-D 100/120, nearly complete and articulated skeleton.

Locality and Horizon—MPC-D 100/125 was collected at Bugin Tsav, western Gobi Desert, Mongolia. The Bugin Tsav locality is situated in the western part of the Gobi Desert and is known as one of the most fossiliferous dinosaur localities in Mongolia (e.g., Barsbold, 1983; Kurochkin and Barsbold, 2000). The Upper Cretaceous Nemegt Formation crops out at this locality (e.g., Gradzinski et al., 1977), consisting mostly of sediments of a meandering fluvial system (e.g., Suzuki and Watabe, 2000; Weishampel et al., 2008). The estimated age of the Nemegt Formation ranges from late Campanian–early Maastrichtian to Maastrichtian (e.g., Gradzinski et al., 1977; Jerzykiewicz and Russell, 1991; Jerzykiewicz, 2000). MPC-D 100/120, on the other hand, was collected at the type locality, Shar Tsav (Watabe et al., 2000).

Revised Diagnosis (Cranial Characters)—*Avimimus portentosus* is distinguished from other oviraptorosaurians on the basis of the following autapomorphies: five denticulations along occlusal margin of premaxilla (as proposed by Kurzanov, 1987); posterior margin of fused nasals strongly concave, surrounding large fossae posteriorly bounded by frontals; quadratojugal thin and long, reaching anterior one-third of orbit; and bones of braincase, squamosal, quadrate, quadratojugal, postorbital, and pterygoid co-ossified.

DESCRIPTION

Referral of MPC-D 100/125 to *Avimimus*

The cranial bones described here were associated with vari-ous, disarticulated postcranial elements presumably belonging to a single individual. Referral of this specimen to *Avimimus portentosus* is based on cranial characteristics listed in the revised diagnosis presented above, including the posterior margin of the fused nasals being strongly concave and the bones constituting the braincase, as well as the squamosal, quadrate, quadratojugal, postorbital, and pterygoid, being co-ossified (Kurzanov, 1981, 1985, 1987; Funston et al., 2016). In addition, the associated postcranial skeleton of MPC-D 100/125 shows diagnostic characters of *A. portentosus* described by Kurzanov (1981, 1987) and Osmólska et al. (2004), including the carpometacarpus and the tarsometatarsus, a large lesser trochanter of the femur separated from the greater trochanter by a wide and deep cleft, and a well-developed medial condyle of the femur.

Braincase and Other Fused Bones

Kurzanov (1981, 1985, 1987) described the braincase of *Avimimus*, particularly a nearly completely preserved one (PIN 3907-3), in detail. Funston et al. (2016) further described the morphology of the posterior part of the braincase based on a specimen (MPC-D 102/81) from Nemegt. Their descriptions are supplemented here with information on the well-preserved braincase of MPC-D 100/125 (Figs. 1–4).

As described by Kurzanov (1981, 1985, 1987) and Funston et al. (2016), the bones constituting the braincase as well as the postorbital, squamosal, quadrate, quadratojugal, and pterygoid are all fused together to produce a single complex (Figs. 1, 2).

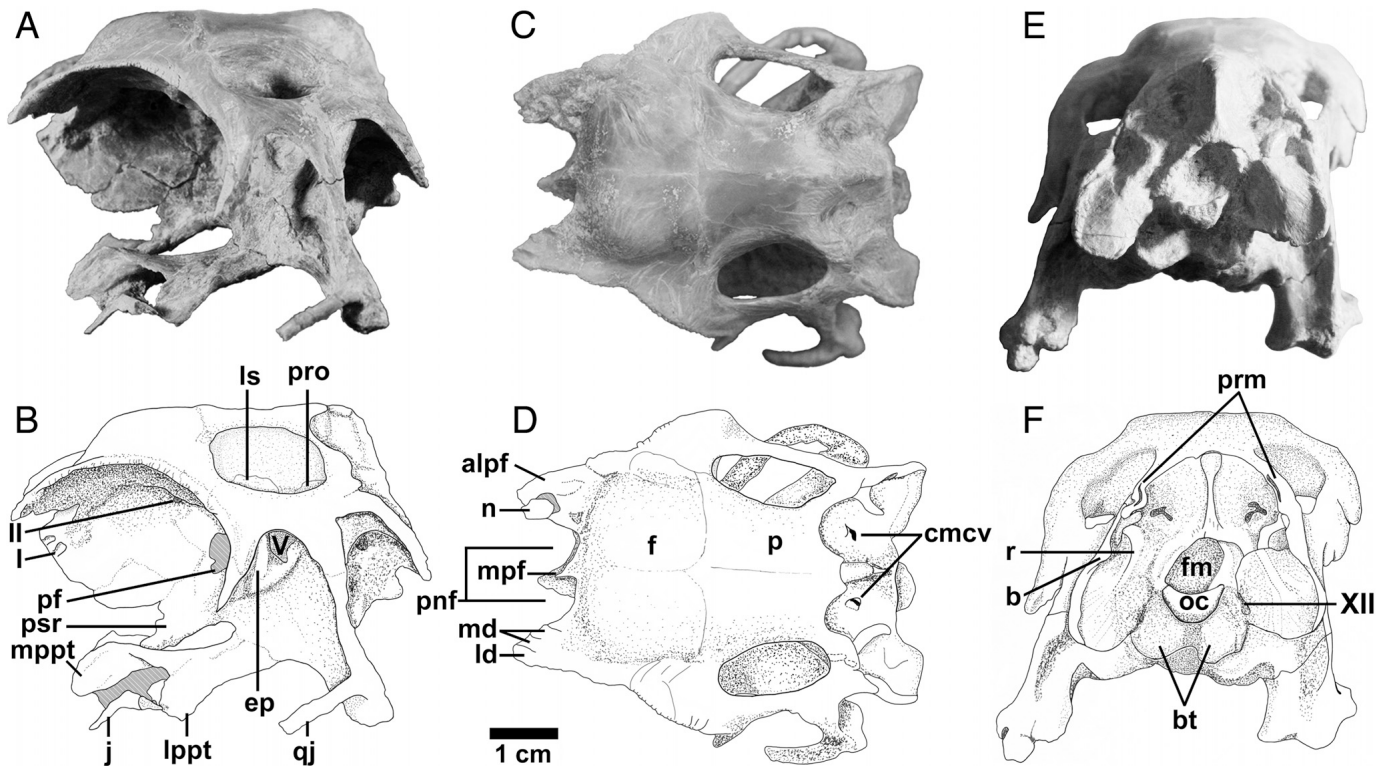


FIGURE 1. *Avimimus portentosus*, MPC-D 100/125, braincase and associated, fused cranial bones. **A**, photograph and **B**, interpretative drawing in left lateral view. **C**, photograph and **D**, interpretative drawing in dorsal view. **E**, photograph and **F**, interpretative drawing in posterior view.

Although the left and right frontals are fused together, the suture between them is still discernible (Fig. 1C, D). The suture between the frontal and parietal is also still visible, whereas the one between the frontal and the postorbital is not discernible dorsally or laterally, unlike Kurzanov's (1985, 1987) description of PIN 3907-3 (Figs. 1C, D, 3C). In ventral view, in contrast, slightly convex lines demarcate the boundary among the frontal, postorbital, and laterosphenoid (Fig. 3D). As emphasized by Kurzanov (1985, 1987), the frontals are inflated dorsally, reflecting the large size of the cerebral hemispheres. A process extends anteriorly from each anterolateral corner of the frontal (Fig. 1C, D). This process bears a sagittal slit medially, followed laterally by two depressions separated by a ridge on the dorsal surface (Fig. 3A, B). The slit and the medial depression are for articulation with the lateral process of the nasal. In fact, a fragment of the lateral process of the nasal is still attached to the right process, fitting within the slit and covering the depression dorsally (Fig. 1C, D). The lateral depression, on the other hand, is likely for articulation with the lacrimal. In addition, the median process of the frontal (which continues ventrally from the bony septum and is fused with the sphenethmoid, separating the left and right olfactory foramina; Figs. 1C, D, 3A, B) would also have articulated with the posterior, median process of the fused nasals. On the lateral surface of this septum, there are two or three longitudinal troughs leading toward each olfactory foramen (Figs. 1A, B, 3B), likely representing the courses of the olfactory nerves. Between the median and lateral processes on each side of the frontal is a deep concavity (Figs. 1C, D, 3A, B), which Kurzanov (1985, 1987) interpreted as the posterior part of the external naris. The discovery of the nasals, and their mode of articulation with the frontal, indicates that this concavity instead likely represents a pneumatic fossa. The orbital margin of the frontal bears 'denticulation' (Kurzanov, 1985) or incising fine grooves that continue posteroventrally along the orbital margin of the frontal

process of the fused postorbital (Figs. 1A–D, 2C). Unlike in most other theropods, there is no fossa on the frontal or postorbital anterior to the supratemporal fenestra.

Unlike in PIN 3907-3 described by Kurzanov (1985, 1987), the descending process of the postorbital is completely preserved on the left side in MPC-D 100/125 (Fig. 1A, B). This process, tapering ventrally, bears an articular facet on the posterolateral surface. Contrary to Kurzanov's (1985, 1987) inference, this facet most likely represents the one for articulation with the jugal, indicating that the orbit is completely separated from the lower temporal fenestra by the postorbital bar. The left and right parietals are fused together (Fig. 1C, D). In dorsal view, the posterior margin of the parietal is embayed anteriorly lateral to the nuchal crest. The dorsal surface of the parietal anterior to this embayment bears shallow grooves, presumably for blood vessels.

The occipital surface of the skull bears various convexities and concavities that likely reflect attachments of soft tissues (Fig. 4). Phylogenetically conserved sites of neck muscle insertions on the occiput among extant diapsids enable robust inferences on such insertion sites in fossil dinosaurs (e.g., Tsuihiji, 2010). Because the paroccipital process extends strongly ventrally, rather than laterally, the relative positions among insertions of the neck muscles in *Avimimus* are superficially similar to those observed in extant birds in most aspects (Fig. 4). The sagittal nuchal crest, which would have served as the attachment of the supraspinal ligament, is well developed, as described by Funston et al. (2016), with its dorsal end forming a tubercle demarcated from the dorsal surface of the parietals (Fig. 1C, D). Lateral to this crest on the occipital surface is a large concavity that would have accommodated the attachments of the medial part of *m. splenius capitis* and *m. complexus* (Fig. 4; Tsuihiji, 2010) as well as a groove of the caudal middle cerebral vein leading to a foramen (e.g., Sampson and Witmer, 2007; Witmer and Ridgely, 2009; Fig. 1C–F). This concavity is bounded laterally by a prominence

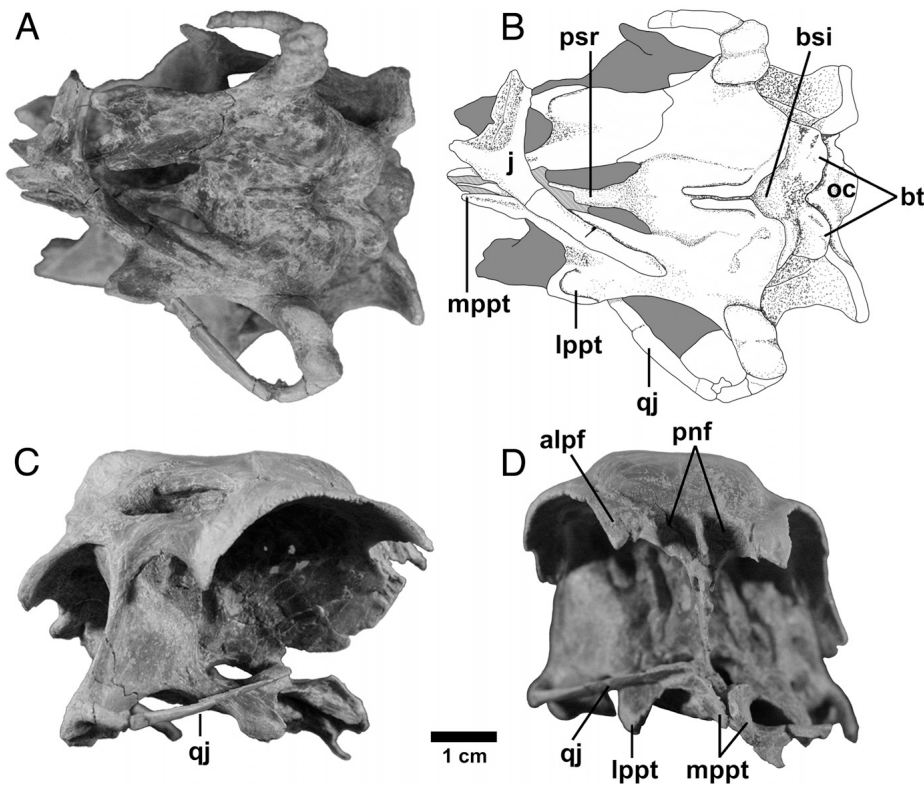


FIGURE 2. *Avimimus portentosus*, MPC-D 100/125, braincase and associated, fused cranial bones. **A**, photograph and **B**, interpretative drawing in ventral view. Photographs showing **C**, right lateral and **D**, anterior views.

bearing a groove extending along the lateral margin of the occipital surface (Fig. 1E, F). This prominence and groove may represent the site of insertion of *m. capitisternalis*, a part of the *m. cucullaris* complex (Fig. 4). An oblique, low ridge extends from dorsolateral to medioventral lateral to the above concavity (Fig. 1E, F). This ridge would likely have separated the insertion of *m. complexus* mentioned above from that of the lateral part of *m. splenius capitis* (Fig. 4). Ventrolateral and adjacent to the ridge is a small depression as well as a boss lying on the lateral margin of the paroccipital process (Fig. 1E, F). Near the foramen magnum, this ridge curves and extends ventrolaterally, dividing the paroccipital process into the dorsolateral and ventromedial surfaces.

The size of the foramen magnum in MPC-D 100/125 is approximately twice that of the occipital condyle even taking the post-mortem deformation into consideration (Fig. 1E, F) and is apparently relatively smaller than the one in PIN 3907-3 but similar in size to the one in MPC-D 102/81 described by Funston et al. (2016). Unlike in *Citipati* but as in many other oviraptorosaurians (Balanoff and Norell, 2012), the neck of the occipital condyle is short and unstricted. As described by Kurzanov (1985, 1987), the paroccipital process curves strongly ventrolaterally (Fig. 1E, F) as in other oviraptorosaurians (e.g., Balanoff and Norell, 2012). The lateral margin of the paroccipital process is thickened.

The basal tubera have an almost vertical orientation. The left and right parts are well separated by a wide notch (Fig. 1E, F). As described by Kurzanov (1985, 1987), the basiptyergoid process of the basisphenoid is low. The pterygoid is completely fused with the quadrate posteriorly. The former is also fused with the basiptyergoid process of the basisphenoid as well as with the bulbous, posterior part of the parasphenoid (Fig. 2A, B). Between the left and right basiptyergoid processes lies a median depression or sinus termed the basal sinus by Kurzanov (1985, 1987), covered ventrally by the pterygoids (Fig. 2A, B). Anterior to this depression, the medial margins of the left and right pterygoids

are thickened, producing a groove between them. More anteriorly, the ventral surface of the pterygoid is concave (or dorsally convex). The anterior end of this bone is divided into short lateral and long medial processes (Fig. 2A, B). The lateral process is tab-like in lateral view (Figs. 1A, B, 2C), representing an articular surface for the ectopterygoid. The medial process similarly forms a dorsoventrally and anteroposteriorly expanded, but mediolaterally thin, articular process for the palatine (Figs. 1A, B, 2C). The parasphenoid is bulbous and pneumatic where it is fused with the pterygoids.

The quadratojugal is posteriorly fused with the quadrate. The remainder of the quadratojugal consists of a thin, elongate process (Fig. 2A–C). It is flattened mediolaterally, although it is more cord-like posteriorly. The jugal would have contacted the quadratojugal laterally as in other oviraptorosaurians such as *Citipati* (Clark et al., 2002) and *Khaan* (Balanoff and Norell, 2012), but unlike in *Rinchenia* (MPC-D 100/321) in which the jugal also contacts the quadratojugal medially, clasping the latter bone between its bifurcated posterior end. On the right side, the quadratojugal appears to be preserved along the entire length, although it is broken at the most posterior part and kinks medially (Fig. 2A–C). If retrodeformed, the anterior end of the quadratojugal would have reached the anterior one-third of the orbit. Despite such length, this structure does not include a fused jugal, contrary to the interpretation by Kurzanov (1985, 1987), as indicated by the presence of a separate jugal in MPC-D 100/125 (see below). Some oviraptorids have an anteriorly elongated quadratojugal, although not to the extent observed in *Avimimus*. In *Citipati*, for example, the quadratojugal extends as far anteriorly as the level of the ascending ramus of the jugal (Clark et al., 2002).

The quadrate is pneumatic as revealed by computed tomography (CT) scan data. The lateral part of the posterior surface of this bone is concave (Fig. 1E, F). The pterygoid ramus of the quadrate and the quadrate ramus of the pterygoid are completely fused together without a discernible suture, forming a laterally convex surface. The articular condyle for the articular

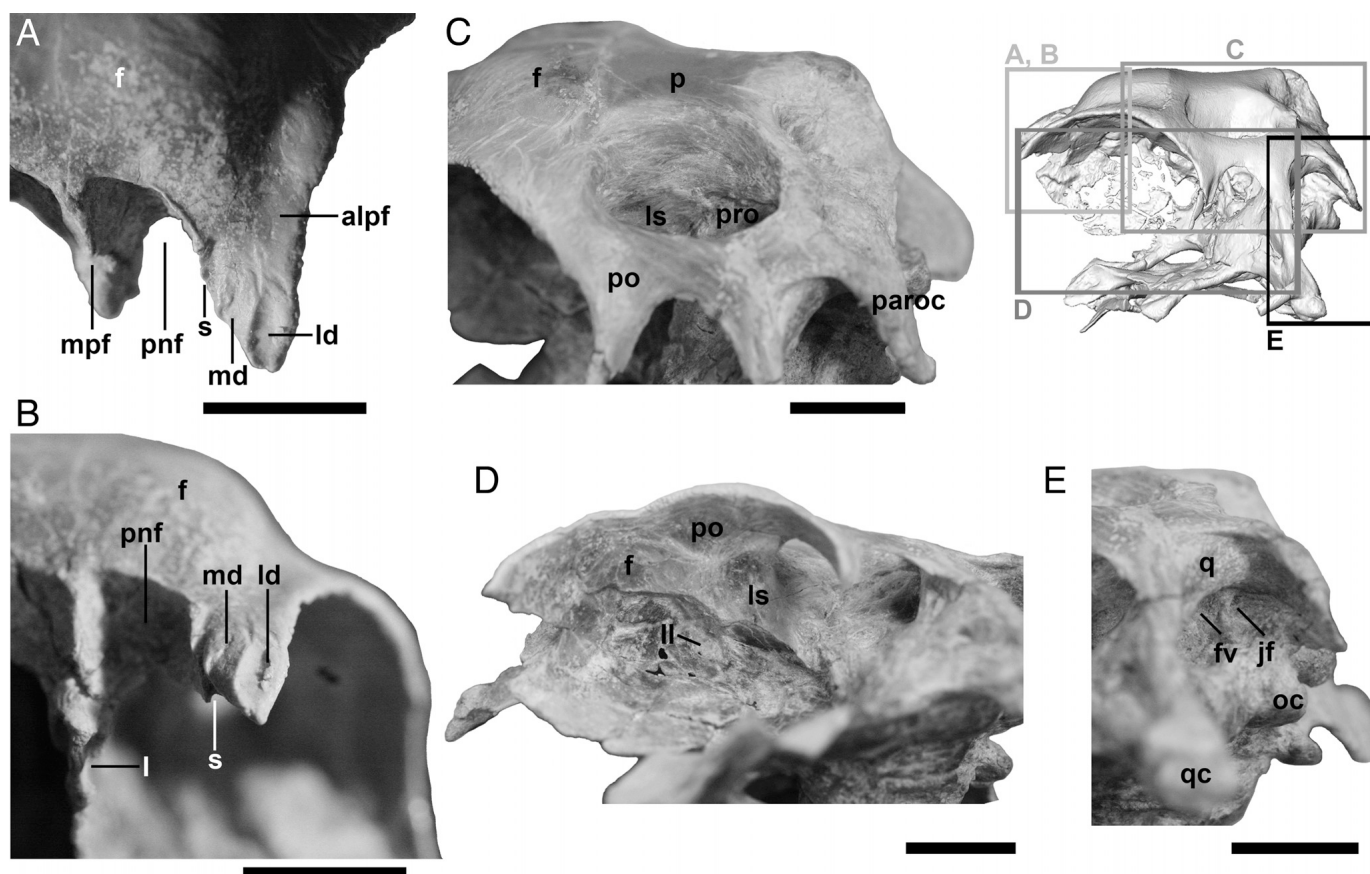


FIGURE 3. *Avimimus portentosus*, MPC-D 100/125, detailed views of braincase. Articular processes of the frontals for the nasals in **A**, dorsal and **B**, anterior views. **C**, region around the upper temporal fenestra in left dorsolateral view. **D**, anterior part of the braincase in left ventrolateral view. **E**, middle ear region in left ventrolateral view. Scale bars equal 1 cm.

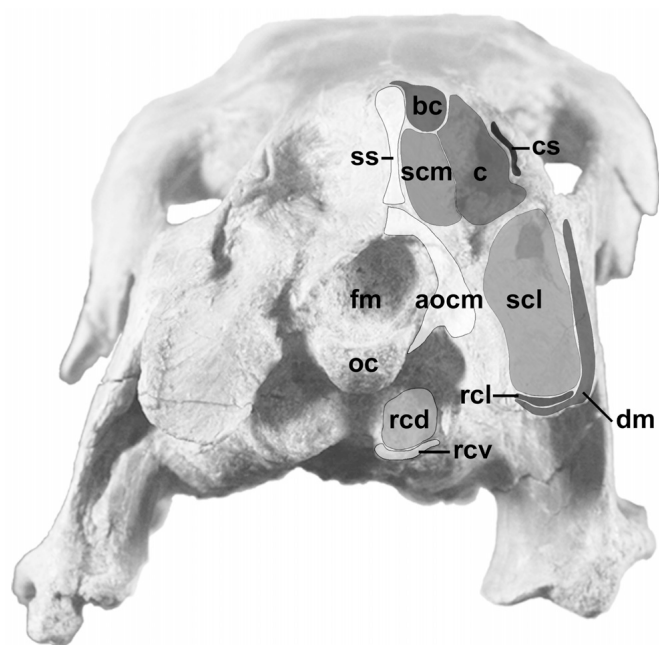


FIGURE 4. *Avimimus portentosus*, MPC-D 100/125, reconstruction of muscle attachments on the occipital region. Names of muscles follow avian nomenclature.

bone is double, with the medial hemicondyle anteroposteriorly more elongated than the lateral one (Fig. 2A, B). Compared with other oviraptorosaurians, including the basal *Incisivosaurus* (Balanoff et al., 2009) and oviraptorids such as *Citipati* (Clark et al., 2002), this condyle lies much more laterally.

The middle ear region of the braincase (putatively consisting of the fused prootic and otoccipital) is generally concave. A deep fossa representing the fenestra vestibuli is present medial to the posteriorly curved dorsal end of the quadrate shaft on the left side (Fig. 3E). Posterior to this fenestra, the jugular foramen or the exit of the glossopharyngeal nerve and associated vasculature is present based on CT images but is visible only on the left side (Fig. 3E).

The lateral aspect of the braincase consists of completely fused bones. However, sutures among the parietal, the laterosphenoid, and the prootic are still discernible (Fig. 1A, B). A possible dorsal tympanic recess is present as a shallow concavity on the prootic near the parietal boundary. A large foramen for the trigeminal nerve is visible, located presumably largely within the prootic and bounded anteriorly by the laterosphenoid, as in diapsids in general (Sampson and Witmer, 2007), and posterior to a vertical bony ridge, which likely represents part of the laterosphenoid and perhaps even a fused epipterygoid (Fig. 1A, B). Foramina for most of the other nerves, except the one for the optic (II) nerve, are not visible on the lateral aspect of the braincase due to breakage of bone. The interorbital septum, consisting of the sphenethmoid dorsally, is thin but extensively developed in front of

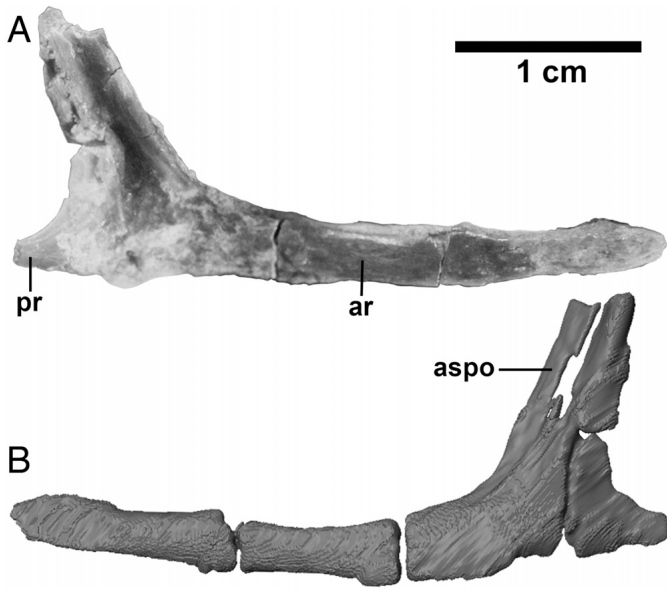


FIGURE 5. *Avimimus portentosus*, MPC-D 100/125, left jugal. **A**, photograph showing medial view; **B**, surface rendering image of lateral view based on CT data.

the braincase region. The pituitary fossa is visible through a large foramen on the interorbital septum above the base of the parasphenoidal rostrum (Fig. 1A, B).

Jugal

The left jugal is preserved in MPC-D 100/125, dislocated from its original position and lying ventral to the palatal bones (Fig. 2A, B), demonstrating that the jugal, previously inferred as fused to the quadratojugal (Kurzanov, 1985, 1987), is a separate bone (Fig. 5). The anterior or maxillary ramus of this bone is dorsoventrally thin and anteroposteriorly elongated, as in many, but not all, other oviraptorosaurians (Balanoff and Norell, 2012). It is only weakly bowed ventrally and tapers at the anterior end. The ascending or postorbital ramus extends posterodorsally, although it is missing the distal end. This ramus is concave along

the medial aspect and bears an articular facet for the postorbital on the anterolateral surface (Fig. 5B). The posterior or quadratojugal ramus is a very short, triangular process. This ramus in other oviraptorosaurians is relatively much more elongated, occupying approximately a half or more of the ventral margin of the lower temporal fenestra (e.g., *Citipati* and *Khaan*; Clark et al., 2002; Balanoff and Norell, 2012).

Nasal

The nasals (Fig. 6) constitute a fused, single element, as recently described by Funston et al. (2016). This condition is similar to that in oviraptorids (e.g., Balanoff and Norell, 2012) but is in contrast to the plesiomorphic, separate condition present in basal oviraptorosaurians such as *Incisivosaurus* (Balanoff et al., 2009) and *Caudipteryx* (e.g., Zhou et al., 2000). The fused nasals consist of a laterally flared main body, an anteriorly extending median premaxillary process, and a posteriorly extending median frontal process, the last one of which was missing in the specimen described by Funston et al. (2016). The latter two processes are continuous with each other on the ventral aspect of the main body (Fig. 6B). The median premaxillary process bifurcates anteriorly and would have clasped the nasal processes of the premaxillae. The specimen described by Funston et al. (2016) indicates that this process is not completely preserved in MPC-D 100/125. The main body consists of very thin bone. The dorsal surface of the main body is smooth (Fig. 6A), lacking a pneumatic foramen as described by Funston et al. (2016). The ventral aspect is generally concave except for the lateral margin and associated processes (Fig. 6B). The anterolateral process of the main body would presumably have articulated with the subnarial process of the premaxilla. This process is short, similar to the one in *Khaan* (Balanoff and Norell, 2012). In *Citipati*, in contrast, this process is longer (Clark et al., 2002). The posterolateral process of the main body was incompletely preserved in specimens described by Funston et al. (2016) but well preserved in MPC-D 100/125. This process ventrally bears an anteroposteriorly extending ridge (Fig. 6B) that would have fit the slit and medial concavity on the dorsal aspect of the anterolateral process of the frontal described above (Fig. 3A, B). The ventral aspect of the lateral margin between the anterolateral and posterolateral processes is an

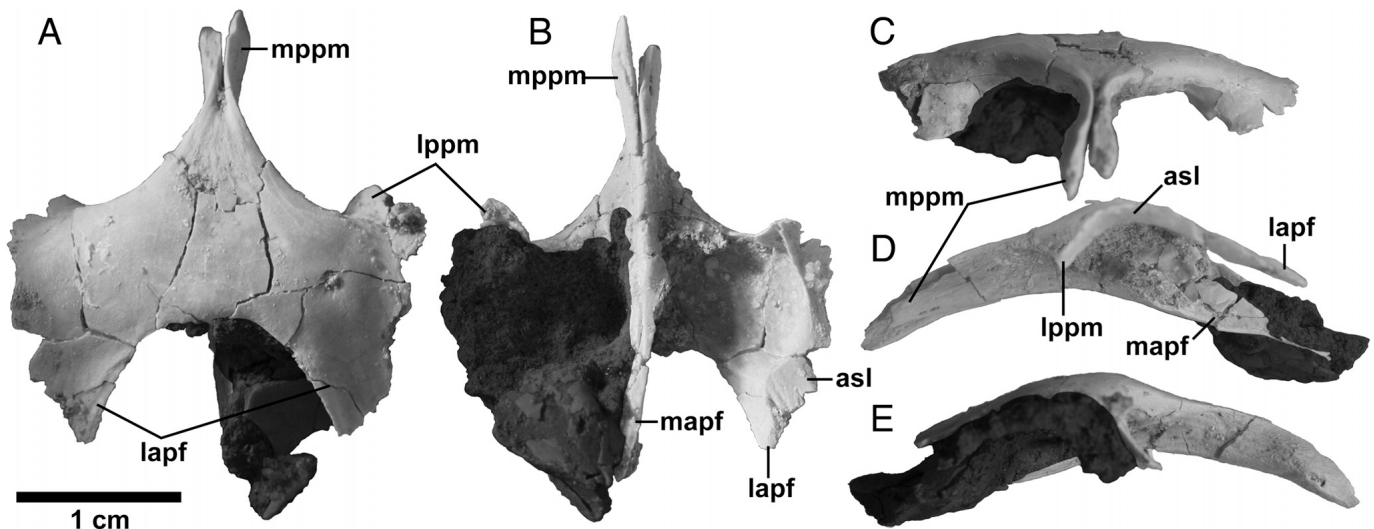


FIGURE 6. *Avimimus portentosus*, MPC-D 100/125, fused nasals. Photographs showing **A**, dorsal, **B**, ventral, **C**, anterior, **D**, left lateral, and **E**, right lateral views. Dark shading indicates attached matrix.

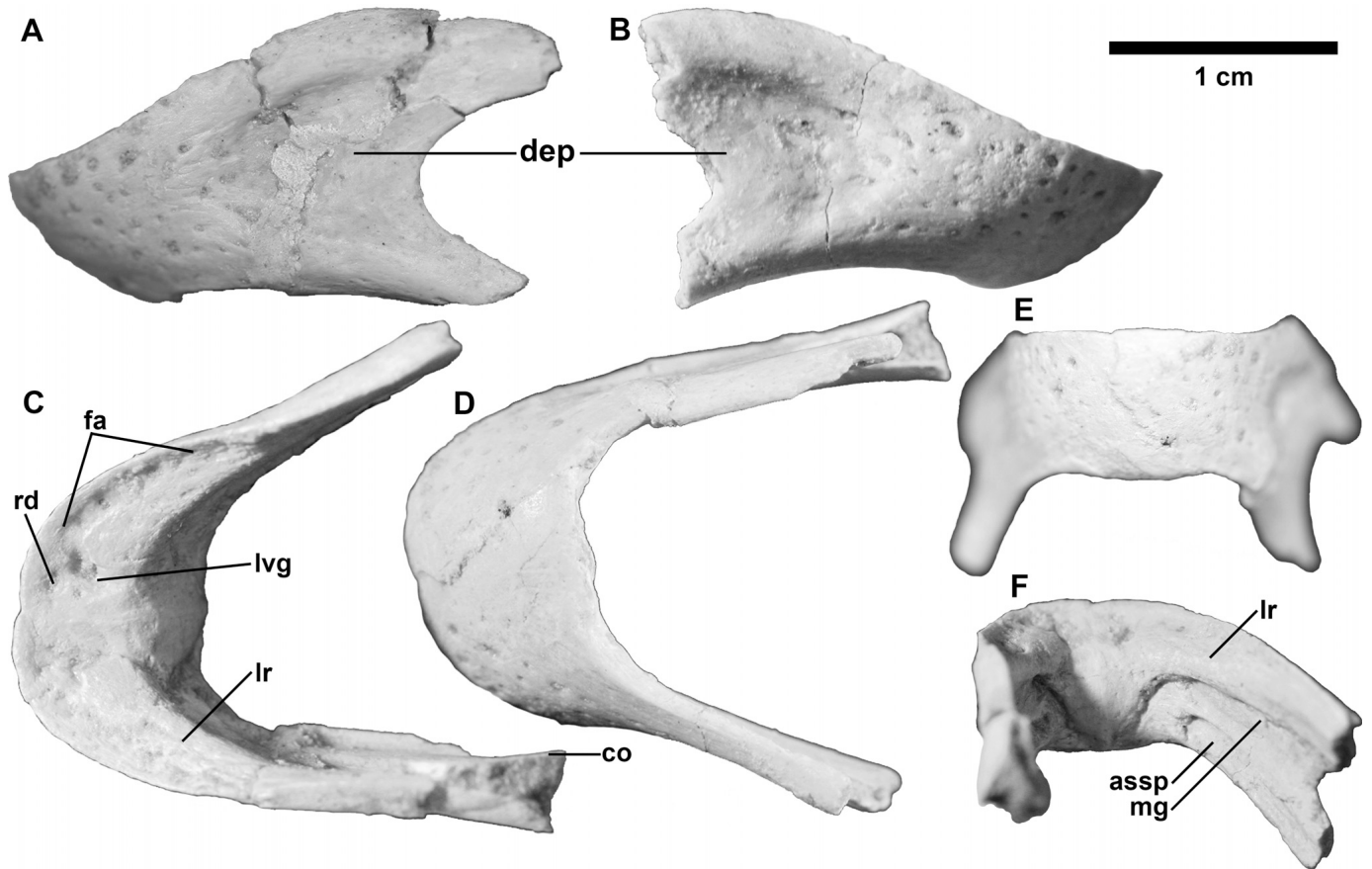


FIGURE 7. *Avimimus portentosus*, MPC-D 100/125, fused dentaries. Photographs showing **A**, left lateral, **B**, right lateral, **C**, dorsal, **D**, ventral, **E**, anterior, and **F**, right posteromedial views.

articular surface for the lacrimal (Fig. 6B). The posterior margin of the main body of the nasals is strongly concave in dorsal or ventral view. This margin, together with the anterior concavity of the frontals, surrounds a large and presumably pneumatic fossa on each side. As described above, the posterior, median frontal process of the nasals is continuous with the anterior premaxillary process along the ventral aspect of the main body (Fig. 6B). The former process would have articulated with the median process of the frontal (Fig. 3A, B), dorsal to the foramina for the olfactory nerves.

Dentary

In addition to a fragmentary left dentary described by Kurzanov (1985, 1987), nearly complete, fused dentaries were described by Funston et al. (2016). The morphology of the dentaries of MPC-D 100/125 (Fig. 7) generally conforms to their descriptions. However, the left and right dentaries of MPC-D 100/125 are apparently completely fused with no trace of a suture, as in caenagnathids (e.g., Currie et al., 1994; Longrich et al., 2013; Lamanna et al., 2014) as well as in *Incisivosaurus* (Xu et al., 2002; Fig. 7). Funston et al. (2016), in contrast, described the dentaries as being only partially fused, preserving a visible suture. As in other oviraptorosaurians, the symphysis is ‘U’-shaped. Teeth are absent. In lateral view, the dorsal or occlusal margin is weakly sinusoidal, with an only slightly concave mesial or anterior part followed distally by the coronoid eminence (Fig. 7A, B). The latter eminence, however, is much less pronounced than those in oviraptorids such as *Citipati* (Clark et al.,

2002; MPC-D 100/42), *Khaan* (Balanoff and Norell, 2012), and *Rinchenia* (MPC-D 100/321). A sharp, beak-like upturning at the mesial end observed in derived caenagnathids (e.g., Currie et al., 1994; Funston and Currie, 2014) is absent. The posterior margin is deeply concave, representing the anterior border of a large external mandibular fenestra. A large depression is present on the labial surface anterior to this margin and ventral to the coronoid prominence (Fig. 7A, B). The mesial-most symphyseal region is devoid of neurovascular foramina and smooth on the labial surface. Such foramina are abundant in the region between the symphysis and the large depression. Unlike the condition described in derived caenagnathids by Currie et al. (1994), these neurovascular foramina do not form any discernible rows.

The ventral aspect of the symphysis lacks the “hourglass- or dumbbell-shaped depression” (Currie et al., 1994:2260) that is present in derived caenagnathids (Fig. 7D). The entire occlusal (dorsal) margin forms a sharp ridge. A lingually extended symphyseal shelf characterizing most oviraptorosaurians is present as described by Funston et al. (2016; Fig. 7C). The lingual ridge (Currie et al., 1994) or triturating shelf (Longrich et al., 2013) continues distolabially or posterolaterally from the symphyseal shelf. The lingual ridge is sharply demarcated ventrally by a longitudinal Meckelian groove, with the ventral margin curving ventrally near the symphysis and bounding mesially a convexity (symphyseal buttress of Funston et al., 2016) that almost reaches the ventral margin of the bone in the midline (Fig. 7F). The Meckelian groove is followed ventrally by another depression representing the articular surface for the splenial.

The middle part of the dorsal surface of the symphyseal shelf is slightly depressed between parasagittal, anteroposteriorly

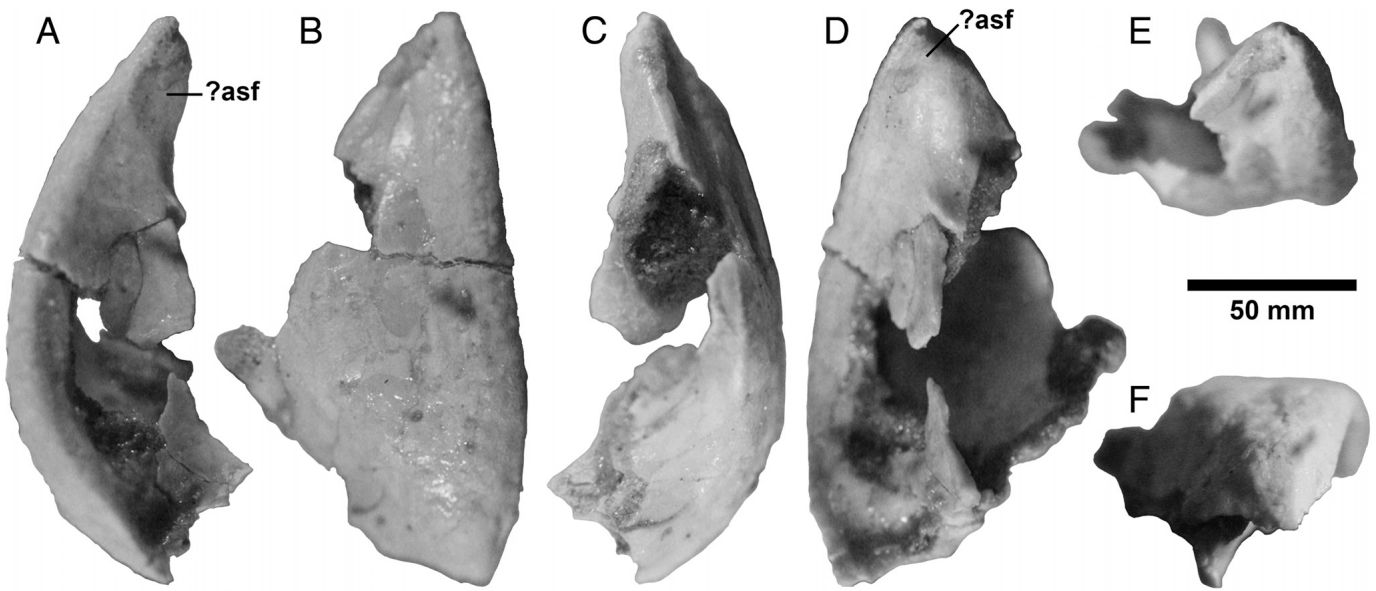


FIGURE 8. *Avimimus portentosus*, MPC-D 100/125, possible left lacrimal. Photographs showing (putatively) **A**, lateral, **B**, anterior, **C**, medial, **D**, posterior, **E**, dorsal, and **F**, ventral views.

elongated depressions corresponding to the longitudinal vascular grooves in Currie et al. (1994; Fig. 7C). Anteromedial to each depression lies another round depression. In addition, at least five foramina lie along the occlusal margin on each side of the dorsal surfaces of the symphyseal shelf and lingual ridge. On the left side, a partial bone, representing the coronoid or a complex of the coronoid, articular, and surangular as in caenagnathids (Currie et al., 1994), is preserved attached to the lingual aspect of the coronoid eminence posterior to the lingual ridge (Fig. 7C). CT-scan data revealed that the inside of the dentaries is hollow and pneumatic, as in caenagnathids (Currie et al., 1994) and unlike the condition reported by Funston et al. (2016).

Other Possible Cranial Bones

There are a few other fragmentary cranial bones found associated with the bones described above. These bones include possible maxilla and lacrimal, although their identifications are ambiguous. The possible left lacrimal is an inflated, hollow element consisting mostly of thin bone, missing the putatively medial and ventral parts (Fig. 8). Dorsally, it ends as a pointed, articular process for the frontal (Fig. 8A, D). The posterior aspect of this process is convex and would have fitted the lateral concavity on the dorsal surface of the anterolateral process of the frontal as described above (Fig. 3A, B). The articular surface for the frontal extends onto the lateral aspect of the bone, demarcated as a slightly

concave surface (Fig. 8A). The rest of the lateral surface is also generally concave except for the anterior margin, which would have formed a laterally convex orbital margin. The anterior surface is convex and lacks any foramina.

A thin plate of bone (Fig. 9) is here tentatively identified as a right maxilla based on the shape of the putative premaxillary articular surface, which is almost flat medially and convex laterally (Fig. 9B) and closely matches the maxillary articular surface of the premaxilla observed in other specimens of *Avimimus* such as MPC-D 100/120 (Fig. 10). The dorsal part that would have housed the antorbital fenestrae is missing. The bone is mediolaterally thickest at the anterior end to produce the premaxillary articular process. The preserved part is dorsoventrally widest at the middle part of the bone, with a convex ventral margin (Fig. 9A, C). The tapering posterior part bears a facet laterally along the dorsal margin presumably for articulation with the jugal (Fig. 9A). The medial surface of the bone is concave and mostly smooth, lacking any trace of the palatine articular process.

DISCUSSION

When Kurzanov (1985, 1987) described the cranial morphology of *Avimimus*, the available cranial bones included braincases, premaxillae, a partial dentary, and a posterior part of the lower jaw. Mainly based on braincase morphology, including

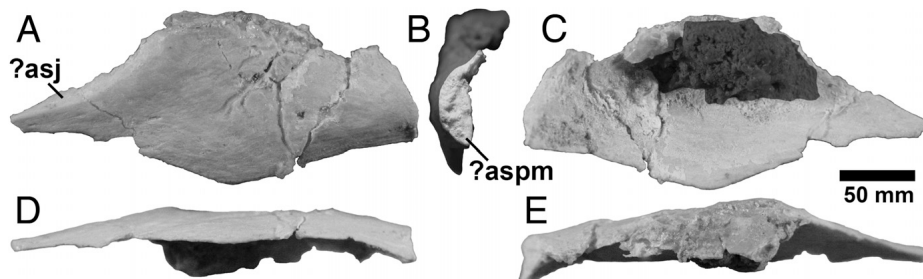


FIGURE 9. *Avimimus portentosus*, MPC-D 100/125, possible right maxilla. Photographs showing (putatively) **A**, lateral, **B**, anterior, **C**, medial, **D**, ventral, and **E**, dorsal views. Putative premaxillary articular surface emphasized by digital darkening of the rest of the bone in **B**. Dark shading indicates attached matrix.

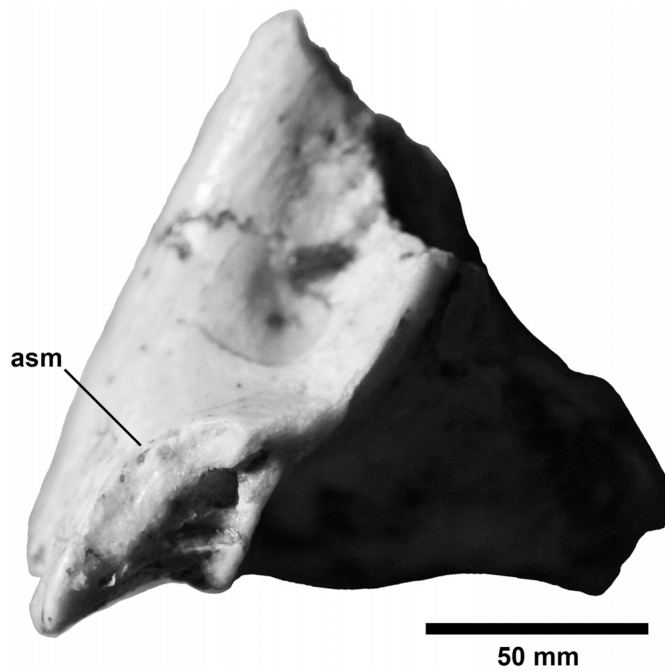


FIGURE 10. *Avimimus portentosus*, MPC-D 100/120, premaxillae from Shar Tsav in left posterolateral view, showing the articular surface for the maxilla.

complete fusion among the comprising bones, Kurzanov (1985, 1987) focused on ‘avian’-like characteristics of the skull, leading to a reconstruction of the entire skull rather peculiar for a non-avian theropod (Kurzanov, 1987:fig. 3). Specimen MPC-D 100/125, described here, includes cranial bones that were not available to Kurzanov (1985, 1987) and reveals several aspects of cranial morphology consistent with oviraptorosaurian affinities of this dinosaur as hypothesized as a result of numerous cladistic analyses (e.g., Osmólska et al., 2004; Turner et al., 2012; Lamanna et al., 2014). First of all, the presence of a separate jugal with a long ascending ramus (Fig. 5) and the morphology of the descending process of the postorbital bearing an articular facet for the jugal indicate the presence of a complete lower temporal fenestra, rather than an incomplete one confluent with the orbit as postulated by Kurzanov (1985, 1987). Second, as recently pointed out by Funston et al. (2016), the morphology of the nasals indicates that the external naris does not extend extremely posteriorly to reach the frontal, contrary to the inference made by Kurzanov (1985, 1987). In addition, as also pointed out by Funston et al. (2016), when articulated with the frontal, the premaxillary process of the nasals extends ventrally at a rather acute angle, suggesting that the snout region is anteroposteriorly shorter and dorsoventrally higher than the reconstruction by Kurzanov (1987:fig. 3). A relatively high and short dentary is also consistent with a short snout, which is a characteristic of most oviraptorosaurians (e.g., Osmólska et al., 2004).

Several characteristics newly observed in MPC-D 100/125 were identified as synapomorphies of subclades of Oviraptorosauria in past analyses. For example, fused nasals were identified as a synapomorphy of Oviraptoridae by Osmólska et al. (2004). In order to examine the effect of new observations on MPC-D 100/125 on the phylogenetic position of *Avimimus*, cladistic analyses were run on the data set of Lamanna et al. (2014) after the coding of characters for this dinosaur was revised. In total, scores of 41 characters were changed or newly coded based on information on MPC-D 100/125 (see Appendix 1 for the list of changed scores). In addition, the score of one character, pneumatization

of the premaxilla (Character 8), was changed from 0 (absent) to 1 (present) based on a CT data set of another specimen of *Avimimus*, MPC-D 100/120, as well as on the description by Funston et al. (2016). Two analyses, one including all of the taxa (41 taxa including 38 oviraptorosaurians) and another excluding caenagnathid taxa without known mandibular material (leaving 34 taxa including 31 oviraptorosaurians), were run based on the revised data matrix. In the first analysis with the all taxa, more than 300,000 most parsimonious topologies were obtained. The strict consensus of these trees (not shown) had very poor resolution, but *Avimimus* was placed more derived than *Incisivosaurus*, *Caudipteryx*, and *Similicaudipteryx*, and more basal than the all taxa that were included in Caenagnathoidea in Lamanna et al. (2014). In the second, culled analysis, 2260 most parsimonious trees were obtained (consistency index [CI] = 0.532, retention index [RI] = 0.685). In the strict consensus of these trees, *Avimimus* was similarly placed between basal taxa (*Incisivosaurus*, *Caudipteryx*, and *Similicaudipteryx*) and Caenagnathoidea, with the latter clade consisting of a polytomy of *Microvenator*, Oviraptoridae, and Caenagnathidae (Fig. 11). Although bootstrap values are rather low for most nodes, this topology is consistent with the strict consensus tree obtained by Lamanna et al. (2014: fig. 6b), but with a much poorer resolution (note, however, that these authors appear not to have conducted further branch swapping starting from the most parsimonious trees obtained in the initial replication, possibly leading to the apparently highly resolved consensus trees shown in their fig. 6). It follows that the revised scoring on *Avimimus* did not alter the inferred phylogenetic position of this dinosaur within Oviraptorosauria.

As an intermediate phylogenetic position between Early Cretaceous basal taxa and the diverse clade of Caenagnathoidea suggests, *Avimimus* shows a mixture of plesiomorphic and derived character states. In order to confirm the phylogenetic distribution of such character states, maximum parsimony character optimization was conducted using MacClade 4.08 (Maddison and Maddison, 2005) based on the revised data matrix and the strict consensus tree obtained in the culled analysis. Only unequivocally optimized nodes are discussed here. One plesiomorphic feature that was retained in *Avimimus* and shared with the basal *Incisivosaurus* is an anteroposteriorly narrow and dorsoventrally high infratemporal fenestra, which is in contrast to a large, anteroposteriorly elongated one (length being comparable to the orbital length) in oviraptorids (Osmólska et al., 2004). On the other hand, fusion of the nasals (Fig. 6), which had been considered as a synapomorphy of Oviraptoridae (Osmólska et al., 2004), was optimized as diagnosing a much more inclusive clade including Caenagnathoidea and *Avimimus*, although all caenagnathid materials included in the analysis lack the nasals (the exact clade that this characteristic diagnoses is dependent on the currently unknown character state and unresolved phylogenetic position of *Similicaudipteryx* in the present tree). Second, a deep fossa on the lateral surface of the dentary (Fig. 7A, B) had been regarded as a synapomorphy of Caenagnathidae, including *Microvenator* and *Gigantoraptor* by Lamanna et al. (2014). Because such a fossa is present in MPC-D 100/125, this characteristic was optimized as having been acquired at least before the divergence between *Avimimus* and Caenagnathoidea and then lost in Oviraptoridae. The presence of a lingual ridge or triturating shelf (Fig. 7C) and pneumatic dentaries had been considered as synapomorphies of a clade consisting of caenagnathids more derived than *Gigantoraptor* in Lamanna et al. (2014). Because both features are present in *Avimimus*, they were optimized as convergently acquired between derived Caenagnathidae and *Avimimus* in the present topology. Similarly, the fused mandibular symphysis (Fig. 7) had been considered as a synapomorphy of *Gigantoraptor* and more derived caenagnathids by Lamanna et al. (2014) and had also been convergently acquired in *Incisivosaurus*. The fused symphysis observed in MPC-D 100/

- Funston, G. F., P. J. Currie, D. A. Eberth, M. J. Ryan, T. Chinzorig, D. Badamgarav, and N. R. Longrich. 2016. The first oviraptorosaur (Dinosauria: Theropoda) bonebed: evidence of gregarious behavior in a maniraptoran theropod. *Scientific Reports* 6:35782.
- Gauthier, J. 1986. Saurischian monophyly and the origin of birds; pp. 1–55 in K. Padian (ed.), *The Origin of Birds and the Evolution of Flight*. Memoir of the California Academy of Sciences 8.
- Goloboff, P. A., J. S. Farris, and K. C. Nixon. 2008. TNT, a free program for phylogenetic analysis. *Cladistics* 24:774–786.
- Gradziński, R., Z. Kielen-Jaworowska, and T. Maryńska. 1977. Upper Cretaceous Djadokhta, Barun Goyot and Nemegt formations of Mongolia, including remarks on previous subdivisions. *Acta Geologica Polonica* 27:281–317.
- Jerzykiewicz, T. 2000. Lithostratigraphy and sedimentary settings of the Cretaceous dinosaur beds of Mongolia; pp. 279–296 in M. J. Benton, M. A. Shishkin, D. M. Unwin, and E. N. Kurochkin (eds.), *The Age of Dinosaurs in Russia and Mongolia*. Cambridge University Press, Cambridge, U.K.
- Jerzykiewicz, T., and D. A. Russell. 1991. Late Mesozoic stratigraphy and vertebrates of the Gobi Basin. *Cretaceous Research* 12:345–377.
- Kurochkin, E. N., and R. Barsbold. 2000. The Russian-Mongolian expeditions and research in vertebrate paleontology; pp. 235–255 in M. J. Benton, M. A. Shishkin, D. M. Unwin, and E. N. Kurochkin (eds.), *The Age of Dinosaurs in Russia and Mongolia*. Cambridge University Press, Cambridge, U.K.
- Kurzanov, S. M. 1981. [On the unusual theropod from the Upper Cretaceous of Mongolia]. *Trudy Sovmestnaya Sovietskogo-Mongol'skaya Paleontologicheskaya Ekspeditsiya* 15:39–50. [Russian]
- Kurzanov, S. M. 1982. [Structural characteristics of the fore limbs of *Avimimus*]. *Paleontologicheskii Zhurnal* 1982:108–112. [Russian]
- Kurzanov, S. M. 1985. [The skull structure of the dinosaur *Avimimus*]. *Paleontologicheskii Zhurnal* 1985:81–89. [Russian]
- Kurzanov, S. M. 1987. [Avimimidae and the problem of the origin of birds]. *Trudy Sovmestnaya Sovietskogo-Mongol'skaya Paleontologicheskaya Ekspeditsiya* 31:5–95. [Russian]
- Lamanna, M. C., H.-D. Sues, E. R. Schachner, and T. R. Lyson. 2014. A new large-bodied oviraptorosaurian theropod dinosaur from the latest Cretaceous of western North America. *PLoS ONE* 9:e92022.
- Longrich, N. R., K. Barnes, S. Clark, and L. Millar. 2013. Caenagnathidae from the Upper Campanian Aguja Formation of West Texas, and a revision of the Caenagnathinae. *Bulletin of the Peabody Museum of Natural History* 54:23–49.
- Maddison, D. R., and W. P. Maddison. 2005. *MacClade: Analysis of Phylogeny and Character Evolution*, version 4.08. Sinauer Associates, Sunderland, Massachusetts.
- Marsh, O. C. 1881. Classification of the Dinosauria. *American Journal of Science* (series 3) 23:81–86.
- Ornitz, D. M., and P. J. Marie. 2002. FGF signaling pathways in endochondral and intramembranous bone development and human genetic disease. *Genes & Development* 16:1446–1465.
- Osmólska, H. 1981. Coossified tarsometatarsi in theropod dinosaurs and their bearing on the problem of bird origins. *Palaeontologia Polonica* 42:79–95.
- Osmólska, H., P. J. Currie, and R. Barsbold. 2004. Oviraptorosauria; pp. 165–183 in D. B. Weishampel, P. Dodson, and H. Osmólska (eds.), *The Dinosauria*. University of California Press, Berkeley, California.
- Owen, R. 1842. Report on British fossil reptiles. Part II. Report of the British Association for the Advancement of Science 11:60–204.
- Sampson, S. D., and L. M. Witmer. 2007. Craniofacial anatomy of *Majungasaurus crenatissimus* (Theropoda: Abelisauridae) from the Late Cretaceous of Madagascar; pp. 32–102 in S. D. Sampson and D. W. Krause (eds.), *Majungasaurus crenatissimus* (Theropoda: Abelisauridae) from the Late Cretaceous of Madagascar. Society of Vertebrate Paleontology Memoir 8. *Journal of Vertebrate Paleontology* 27(2, Supplement).
- Suzuki, S., and M. Watabe. 2000. Report on the Japan-Mongolia Joint Paleontological Expedition to the Gobi Desert, 1995. *Hayashibara Museum of Natural Sciences Research Bulletin* 1:45–57.
- Tsuihiji, T. 2010. Reconstructions of the axial muscle insertions in the occipital region of dinosaurs: evaluations of past hypotheses on Marginocephalia and Tyrannosauridae using the Extant Phylogenetic Bracket approach. *Anatomical Record* 293:1360–1386.
- Turner, A. H., P. J. Makovicky, and M. A. Norell. 2012. A review of dromaeosaurid systematics and paravian phylogeny. *Bulletin of the American Museum of Natural History* 371:1–206.
- Vanden Berge, J. C., and G. A. Zweers. 1993. Myologia; pp. 165–183 in J. J. Baumel, A. S. King, J. E. Breazile, H. E. Evans, and J. C. Vanden Berge (eds.), *Handbook of Avian Anatomy: Nomina Anatomica Avium*. Nuttall Ornithological Club, Cambridge, Massachusetts.
- Vickers-Rich, P., L. M. Chiappe, and S. Kurzanov. 2002. The enigmatic birdlike dinosaur *Avimimus portentosus*: comments and pictorial atlas; pp. 65–86 in L. M. Chiappe and L. M. Witmer (eds.), *Mesozoic Birds: Above the Heads of Dinosaurs*. University of California Press, Berkeley, California.
- Watabe, M., D. B. Weishampel, R. Barsbold, K. Tsogtbaatar, and S. Suzuki. 2000. New nearly complete skeleton of the bird-like theropod, *Avimimus*, from the Upper Cretaceous of the Gobi Desert, Mongolia. *Journal of Vertebrate Paleontology* 20(3, Supplement):77A.
- Weishampel, D. B., D. E. Fastovsky, M. Watabe, D. Varricchio, F. Jackson, K. Tsogtbaatar, and R. Barsbold. 2008. New oviraptorid embryos from Bugin-Tsav, Nemegt Formation (Upper Cretaceous), Mongolia, with insights into their habitat and growth. *Journal of Vertebrate Paleontology* 28:1110–1119.
- Witmer, L. M., and R. C. Ridgely. 2009. New insights into the brain, braincase, and ear region of tyrannosaurs (Dinosauria, Theropoda), with implications for sensory organization and behavior. *Anatomical Record* 292:1266–1296.
- Xu, X., Y.-N. Cheng, X.-L. Wang, and C.-H. Chang. 2002. An unusual oviraptorosaurian dinosaur from China. *Nature* 419:291–293.
- Yu, K., A. B. Herr, G. Waksman, and D. M. Ornitz. 2000. Loss of fibroblast growth factor receptor 2 ligand-binding specificity in Apert syndrome. *Proceedings of the National Academy of Sciences of the United States of America* 97:14536–14541.
- Zhou, Z.-H., Z.-L. Wang, F.-C. Zhang, and X. Xu. 2000. Important features of *Caudipteryx*—evidence from two nearly complete new specimens. *Vertebrata Palasiatica* 38:241–254.

Submitted September 28, 2016; revisions received May 29, 2017; accepted June 18, 2017.

Handling editor: Alan Turner.

